OPEN ACCESS

Experimental Study of Jet Control with Ventilated Triangular Tabs

Utkarsh Dadhich[1], Rakhab C. Mehta[2*] and E. Rathakrishnan[1]

[1]Department of Aerospace Engineering, Indian Institute of Technology Kanpur, India
[2]Department of Aeronautical Engineering Noorul Islam Centre for Higher Education, Kumaracoil, India

Abstract	Original Research Article

The results of a Mach 1.5 elliptical jet issuing from a convergent divergent elliptical nozzle of aspect ratio 3, controlled with two triangular tabs of 2.5% blockage each are presented. The decay for the jets with tabs located at the extremities of the major and minor axes are compared for different nozzle pressure ratio NPR 3, 4, 5, and 6. The decay of the uncontrolled jet and without tabs is also included for comparison. It is seen that among the tab orientations, placing along the minor tabs along minor axis is found to be the best mixing promoter resulting in 80% and 74% core length reduction, respectively, at NPR 3 and NPR 4. At NPR 6, the ventilated triangular tabs with circular holes on major axis and triangular tabs with triangular holes on minor axis are found to be more effective in enhancing the mixing. The triangular tabs used in present study is special in the sense that it is capable of producing mixing promoting vortices of continuously varying size, in accordance with the vortex theory, unlike conventional rectangular tabs which will shed mixing promoting vortices of uniform size only. For all the cases, tabs along minor axis promotes mixing and tabs along major axis retard the mixing. Among the ventilations studied, the circular hole is found to be superior to the triangular hole. This superiority of circular ventilation is found to be independent of the expansion level at the nozzle exit.
Keywords: Experimental Study, Ventilated Triangular Tabs, Nozzle, Gas Dynamics, Supersonic jets.

INTRODUCTION

Jet is a free shear flow driven by momentum introduced at the exit of, usually, a nozzle which exhibits a characteristic that, "the ratio of width to axial distance is a constant (B/X = constant)". The value of this constant is 8, for Mach number less than 0.2, and decreases with increase of Mach number. Alternatively, a jet may also be defined as a fluid flow on either side of the tangential separation surfaces. Free jets can be defined as a pressure driven unrestricted flow of a fluid into a quiescent ambiance. Since a fluid boundary cannot sustain a pressure difference across it, the jet boundary is a free shear layer, in which static pressure is constant throughout, when the jet is subsonic. The boundary layer at the exit of the nozzle, on exiting develops as a free shear layer, mixing with the ambient fluid, thereby entraining the ambient fluid into the jet stream [1]. Thus, mass flow at any cross-section of a jet progressively increases along the downstream direction. In other words, it can be stated that continuity equation is not valid for the jets. Hence, to conserve momentum the centerline velocity decreases with downstream distance. The vast quanta of knowledge presently available and the continuous research currently being carried out stand testimony to the importance associated with the jet flows. This is owing to their extensive nature of applicability, from household appliances to space technology. High-speed jets find application in numerous engineering fields; aircraft, rockets, missile, propulsive systems of aircraft and thrust augmenting ejectors. The experimental studies on jets will be provided insight into the understanding of the dynamics of free shear layers and vortical structures.

Classification of Jets

Basically, jets can be classified into two categories namely, incompressible and compressible jets. The jets with Mach number less than 0.3 up to which the compressibility effects are negligible are called incompressible jets. Compressible jets can be again subdivided into subsonic, sonic and supersonic jets. Jets with Mach number 1.0 are called sonic jets which can be correctly expanded or under expanded. Supersonic jets are the jets with Mach number more than one. These can be further classified into over expanded, correctly expanded and under expanded jets as shown in Figure-1. The jets flow characteristics are

investigated by many researchers in [2 – 23] and reviewed in the following sections.
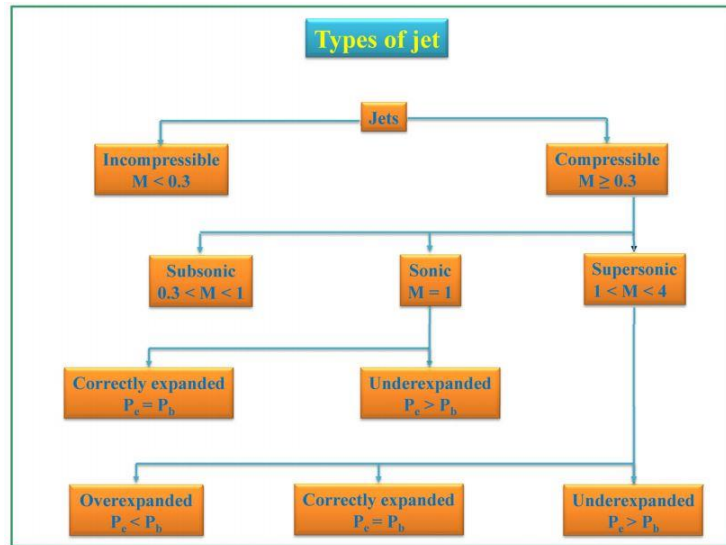
Fig-1: Classification of Jets

Subsonic Jets

A schematic diagram of a typical subsonic jet and the different flow zones in it are shown in Figure-2. These are jets with Mach numbers from 0.3 to 0.8, and flow regimes are classified into the following categories.

Potential core region: Here, the mixing initiated at the jet boundaries has not yet permeated into the entire flow fields, thus leaving a region that is characterized by a constant axial velocity, just downstream of the nozzle exit. The profile takes a "top-hat" shape at the nozzle exit as depicted Figure-2. Due to absence of vorticity, this region is essentially inviscid and hence termed potential region.

In subsonic jets, the potential core region is defined the extent up to which axial velocity is constant.

However, in supersonic jets there is no constant axial velocity zone exists because of wave domination. Therefore, the supersonic core is defined as the axial extent up to which waves dominate. In other words, the axial extent from the nozzle exit to the beginning of characteristics decay zone.

Transition region: Herein the axial velocity decay is dependent upon nozzle configuration, and the velocity profiles become smoother with jet propagation.

Fully developed region: Beyond the transition region the jet becomes similar in appearance of to a flow of fluid from a source of infinitely small thickness (in axially symmetric case the source is a point, and in a plane parallel case it is a straight line perpendicular to the plane of the flow of the jet). In reality the jet velocity becomes insignificant after about 30D.
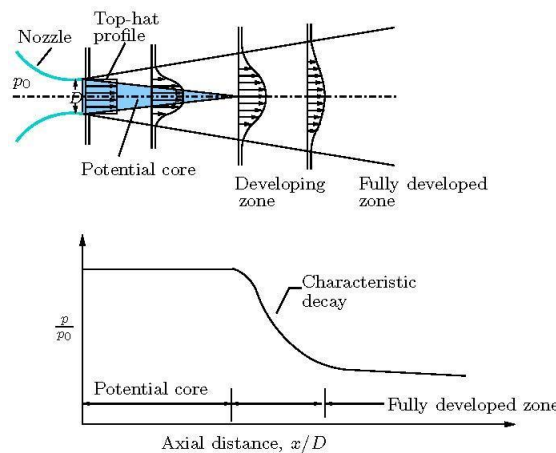
Fig-2: Schematic view of the different zones in the development of a subsonic jet

Over Expanded Jets

If the pressure in the ambient medium to which the jet is discharging is greater than the nozzle exit pressure, the jet is said to be over expanded. In this case, oblique shock waves are formed at the edge of the nozzle exit. These oblique shock waves will be reflected as expansion waves from the boundary of the jet. Figure-3 schematically shows the waves prevailing in an over expanded jet. Due to these waves, a periodic shock cell structure is generated in the jet and the length of these periodic structures is found to increase with Mach number. For an over expanded jet, nozzle exit pressure, p_e, is lower than the ambient pressure, p_a. This causes an oblique shock to form at the nozzle exit plane. To approach equilibrium with the ambient pressure, the exhaust gas undergoes compression through the oblique shock waves standing at the exit plane. Flow that has passed through the shock waves will be turned toward the centerline. At the same time, the oblique shock wave, directed toward the centerline of the nozzle, cannot penetrate the center plane as a linear wave-front, since it encounters the wave from the opposite lip of the nozzle. On passing through the shock from the opposite direction, it gets deflected as shown in the figure. The gas flow goes through these reflected shocks and is further compressed, but the flow is now turned parallel to the centerline. This causes the pressure of the exhaust gases to increase above the ambient pressure. Deflected shock wave now hits the free jet boundary (or the boundary where outer edge of the gas flow meets the freestream air).
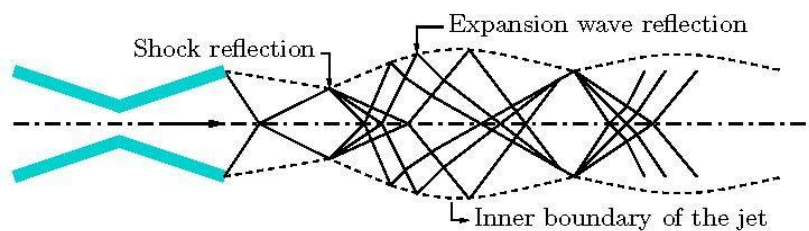

Fig-3: Schematic of the waves prevailing in an over expanded jet

Correctly Expanded Jets

A jet is said to be correctly expanded when the nozzle exit pressure is equal to the ambient pressure. This jet is also wave dominated, as is an imperfectly expanded jet, even though we might think that there would not be any waves. The reason for this is that, as the jet is issuing from a confined area to an infinite area, it tries to expand through expansion waves and after that gets compressed through compression waves (the reflected waves from the jet boundary), which results in a periodic wave structure.

Under expanded Jets

If the pressure in the ambient medium (backpressure) is lower than the nozzle exit pressure, the jet is said to be under expanded. Since the back pressure is less than the nozzle exit pressure ($p_e < p_b$), wedge-shaped expansion waves occur at the edge of the nozzle. These waves cross one another and are reflected from the opposite boundaries of the jet as compression waves. The compression waves again cross one another and are reflected on the boundaries of the jet as expansion waves. The under expanded jets are further classified as moderately and highly under expanded. In the moderately under expanded jets, the meeting of compression waves from one side of the nozzle with the waves of opposite family at the jet centerline forms the cross-over point at the end of first shock cell as depicted in Figure 4. Whereas, in highly under expanded jets, these waves do not meet but are reflected though the edges of a normal shock disk termed as "Mach disk" as shown in Figure-4 [24].
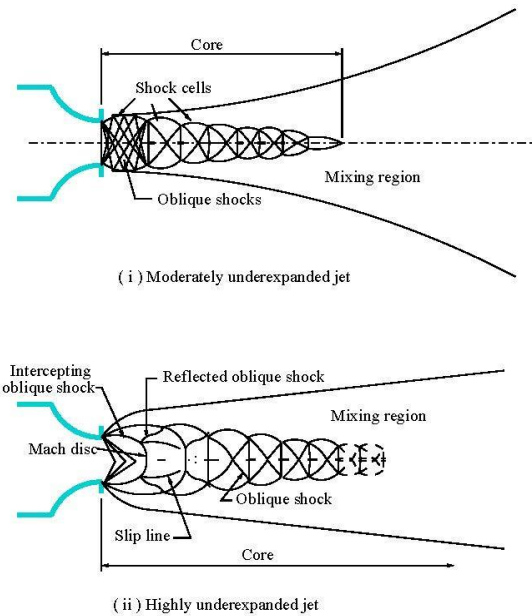
(i) Moderately underexpanded jet

(ii) Highly underexpanded jet

Fig-4: Schematic of the waves prevailing in an under expanded jet

Need of Jet Control

The ability to enhance the mixing of a jet will greatly improve the performance of a large number of devices. For example, by increasing the rate of mixing between air and fuel, the efficiency of a combustion cycle can be improved. In scramjet the entire mixing process has to be completed within a short distance to minimize the size of the combustor and for enhancing the performance of the entire vehicle system. In combustion systems, both large- and small-scale mixing enhancement is sought since large-scale mixing determines the rapidity of the mixing process and small scale or micro scale mixing ensures effective molecular level mixing for efficient combustion. By increasing the rate of mixing with the ambient, the infrared radiance of the plume can be reduced. Other examples of technological applications requiring control of mixing in compressible flows include thrust augmenting ejectors, thrust vector control, metal deposition and gas dynamic lasers. The diverse nature of applicability of jets demands that they be made suitable for a specific application by controlling them. Here, control may be defined as the ability to modify the jet flow mixing characteristics to achieve engineering efficiency, the technological ease, economy, adherence to standards and so on.

Types of Control

All types of jet controls can be broadly classified into active and passive controls. In active control, an auxiliary power source (like micro jets) is used to control the jet characteristics. In passive control the controlling energy is drawn directly from the flow to be controlled. Both active and passive controls mainly aim at modifying the flow and noise characteristics.

Active Control

Many active jet control methods use energized actuators to dynamically manipulate flow phenomena by employing open- or closed-loop algorithms. Pulsed jets, piezoelectric actuators, micro jets and oscillating jets are among the most effective controls for active mixing enhancement. The design of an active flow control system requires knowledge of flow phenomenon and selection of appropriate actuators, sensors and a control algorithm. The role of an actuator is to inject perturbations at a prescribed frequency into the flow at locations where the flow is most receptive to these inputs. The actuator leverages or disrupts the flow to bring about a desired effect. For example, the conventional excitation methods rely on exciting instability modes with their most amplified frequency band to bring about jet mixing enhancement. For jet excitation, the conventional philosophy has been to energize the large-scale coherent structures (large suction creators) or bring about vortex interactions that result in the engulfment of surrounding fluid (entrainment), resulting in mixing enhancement.

Passive Control

Among the two main types of control, passive controls are mostly desired not only because no external power source is required, but since in some cases engineer is left with no other option. Passive control methods use geometrical modifications which alter the flow structure. Some of the commonly used passive control methods are shown in Figure-5.
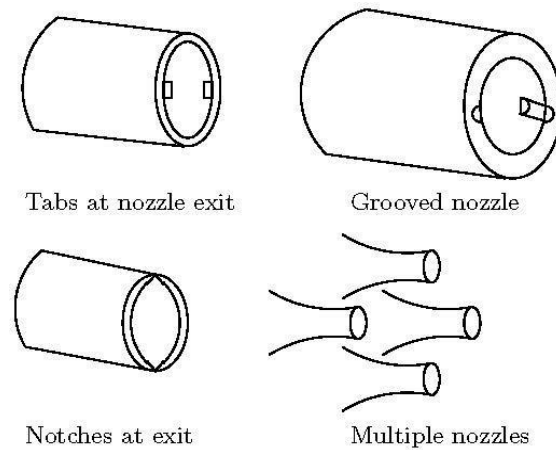
Fig-5: Schematic of few passive controls

Tabs at nozzle exit   Grooved nozzle

Notches at exit   Multiple nozzles

Passive control techniques range from alterations in the exit shape of nozzle to the implementation of tooth like tabs and vortex generators in the jet. Many studies have focused on the placement of small tabs and vortex generators at the exit of axisymmetric and rectangular nozzles. These methods primarily aim at disturbing the boundary layer at the nozzle exit to achieve the desired flow behavior. Particularly, the grooves and tabs at the exit trip the boundary layer developing inside the nozzle. This drastically influences the shear layer growth and flow behavior, thus providing a lot of scope for mixing enhancement.

Review of mixing enhancement techniques in jets

The present work aims at investigating the effects of varying corrugation geometries to control the mixing characteristics of a Mach 1.5 jet in the presence of adverse and favorable pressure gradients.

A significant amount of research is currently being performed on mixing enhancement in compressible shear layers and jets. The cause for reduced mixing (increased stability) with increasing compressibility and ways to counteract the effects of compressibility on decreased mixing remains relatively unexplained. Compressible mixing flows are encountered in many situations with the two main driving applications, namely the combustion efficiency in high- speed propulsion systems and reducing noise emission by high-speed jets. Both are serious concerns, directly related to the decreased mixing in compressible mixing layers. These issues must be addressed before the next generation of high-speed aircraft can be made economically and environmentally viable. Mixing is also important in the performance of supersonic ejectors, which play a crucial role in chemical lasers, entrainment of metal powders into supersonic jets for metal deposition [7], and in noise and infra-red signature detection for supersonic military aircraft [8,9]. The technological challenge of mixing enhancement in compressible flows stems from the inherently low growth rates of supersonic shear layers. Many mixing augmentation methods employed efficiently in subsonic

flows failed to work at elevated Mach numbers. Some of these methods were inefficient because they were utilized outside their effective range. Nevertheless, studies of compressible shear flows are built on the knowledge accumulated in subsonic flow research. The discovery of large-scale coherent structures in subsonic shear layers and their importance to the mixing process led the development of numerous mixing control techniques.

The original work of Brown and Roshko [10] on the structure of planar mixing layer triggered extensive research during the past three decades that substantiated the idea that large-scale coherent structures control the dynamics of all free shear flows including plane mixing layers, jets of different geometries (axisymmetric, plane, elliptic, rectangular and so on) and wakes. These two-dimensional structures were found to play an important role in entrainment and mixing processes in incompressible shear layers.

The formation of coherent structure in shear layer is initiated by Kelvin Helmholtz instability, governed by Rayleigh's equation for inviscid flows. The exponential growth of the velocity and vorticity perturbations leads to a nonlinear process that eventually causes the roll-up of shear layer vortices. The initial vortex shedding frequency also called the most amplified frequency is determined by various characteristics of the exit velocity profile such as shape, turbulence structure, initial shear layer momentum thickness, and the jet exit velocity (U_0).

The initial vortices grow in the shear layer and coalesce as they are convected downstream in a `pairing' process. Due to merging and entrainment, the shear layer spreads, and the frequency associated with the large vortices decreases. The irrotational entrainment by the large-scale structures leaves the entrained fluids essentially unmixed during the lifetime of the vortices [11]. Nonetheless, intense mixing occurs during pairing or other amalgamation processes. Some distance downstream of the splitter plate trailing edge, a secondary, span wise instability appears, leading to the

development of streamwise vortices [12]. The appearance of these vortices enhances the mixing process, which is referred to as the `mixing transition'. The streamwise vorticity, which is organized in `ribs', interacts with the span wise structures. With increasing downstream distance, the interaction increases the three-dimensional structure in the shear layer leading to high-order instabilities and transition to small-scale dominated flow.

The central techniques used to achieve this excitation are broadly classified as passive and active controls. Passive controls, which uses geometrical modifications of the element from which flow separation occurs to change the shear layer stability characteristics. Some examples of these modifications are: trip wires in plane shear layers, convoluted splitter plates, non-circular jets such as square jets [14], rectangular jets, and elliptic jets [8]. Some additional passive techniques in non-reacting and reacting flows were reviewed by Gutmark *et al.*, [15].

The other approach to control involves external forcing and is called active control. These methods are selected to achieve maximum receptivity for the specific medium considered. The flow can be excited by mechanical means such as fluctuating flaps, vibrating ribbons, piezoelectric surfaces, acoustical perturbation, hydrodynamic methods such as periodic suction and blowing, thermal techniques such as heating strips or electrical discharge, or by the modulation of the free stream. To maximize the effect, the external perturbations should match the flow instability band to take advantage of the natural amplification of the flow. Crow and Champagne [13] demonstrated active control of a turbulent jet. They used acoustical excitation at the preferred mode of the jet to enhance the jet's growth rate and produce highly coherent structures. By choosing the proper frequency, the growth rate and entrainment characteristics of the shear layer can be controlled to either enhance or suppress them.

Mixing in supersonic shear layers is critically dependent upon the compressibility effects in addition to the velocity and density ratios across the shear layer. The compressibility level is best described by a parameter called the convective Mach number (Mc) [9, 16]. This parameter is defined as the relative convection speed of the large-scale structures in shear layer to one of the freestreams, normalized by the speed of sound of that stream. The two convective Mach numbers of the streams (designated as 1 and 2) are: $M_{c1} = (U_1 - U_c)/ a_1$ and $M_{c2} = (U_2 - U_c)/ a_2$, where "$U_c$" is the convective velocity of the structures, U is the mean velocity of the freestream, and a is the speed of sound. These convective Mach numbers are equal to each other in shear layers with equal static pressures and specific heat ratio in the two streams, $M_{c1} = M_{c2} = M_c = (U_1 - U_2)/(a_1 + a_2)$.

The ratio of compressible to incompressible spreading rates of the shear layer has been described as a function of the convective Mach number. The compressibility effects cause the spreading rate to drop significantly, reaching an asymptotic value close to 20 percent of the spreading observed in incompressible shear layers, for $M_c > 0.8$. One potential mechanism for the stabilization of the compressible shear layer, relative to incompressible flow, is the suppression of upstream and cross-flow communication paths within the shear layer due to the high Mach number [9]. Acoustic interaction between different regions of the shear layer, possible in an elliptic subsonic flow, is inhibited, thus stabilizing the compressible flow.

Non-circular jets, such as rectangular and elliptic jets, due to the continuous variation in radius of curvature, form flow structures of different sizes at the jet boundary and the jet spreads differently along different planes [4, 5]. Various previous studies on non-circular jets show that the jet produces fine scale mixing at the corners or high curvature regions and is good suction creators at the low curvature/flat side regions resulting in high entrainment [2, 17]. Extensive research has been done on square and rectangular jets in the past several decades. Rectangular slot jets ($M_j = 1.4 – 1.8$) exhibit large spreading rates when operating at moderately under expanded conditions [18, 19]. At this range, the jet generates intense discrete tones called screech. The interaction of these tones with the jet's shear layer results in the formation of large- scale vortices which develop alternatively on the two sides of the jet along its wide side. The resulting flapping motion yields a high spreading rate and accelerates the mixing process. Rectangular supersonic jets with various designs of the divergent section of the nozzle were tested over a wide range of convective Mach numbers ($0.5 < M_c < 2.2$) by Gutmark *et al.*, [5].

The nozzle design with internal divergence along the wide side of the nozzle increased the spreading rate by a factor of 2 throughout the entire range of $M_c < 1.8$. Srinivasan *et al.*, [20] carried out experimental studies on rectangular slot jets aspect ratio 1, 2, 4 and 6, in sonic and under expanded conditions, with an aim of understanding the core region of the jet, particularly the pitot pressure oscillations in the core. The results show that, aspect ratio is a crucial parameter for rectangular jets. The amplitude of pressure oscillations showed a monotonic variation for aspect ratio 1:1 and 2:1 rectangular jet, and an oscillatory variation for aspect ratio 4:1 and 6:1 jet, indicating possibility of entirely different mechanisms in the jet core for lower aspect ratio and higher aspect ratio rectangular jets.

However, elliptic jets have not received much attention like square and rectangular jets. The limited number of studies reported on elliptic jet clearly demonstrates their superior mixing capabilities

compared to circular jets. The enhanced mixing capability of elliptic jets compared to their circular counterpart is due to the generation of azimuthal vortices of continuously varying size generated at the nozzle exit [6]. These mixed size vortices promote both large and small-scale mixing. Whereas in circular jets, the curvature is same across the jet boundary, therefore the mixing is not as rapid as in elliptic jets. Earlier studies on elliptic jets support this fact. Schadow *et al.*, [21] studied an elliptic jet of aspect ratio 3:1 and found enhanced mixing characteristics of the elliptic jet compared to a circular jet at subsonic, sonic and supersonic under expanded conditions. Quinn [3] showed that mixing in an elliptic jet issuing from a sharp-edged orifice plate is higher than in elliptic jets issuing from contoured elliptic nozzles and in round jets. Mitchell *et al.*, [22], using planar particle image velocimetry studied a low aspect ratio under expanded elliptical jet and reported a vortex bifurcation process at the highest-pressure ratio of NPR = 4.2, which was previously observed only for jets with higher aspect ratio. Yoon and Lee [23] investigated the near field structure of an elliptic jet using stereoscopic particle image velocimetry and reported that the total entrainment rate of the elliptic jet was about 1.5% larger than that of the round jet.

The enhanced mixing of elliptic jets is reflected in the form of axis-switching. In axis-switching the major- and minor-axis of jet switch after a certain distance downstream of the nozzle exit. Many researchers have observed axis-switching. Hussain and Husain [24] observed that the locations and number of axis-switching were strongly dependent on the initial conditions of the jet. Ho and Gutmark [25] reported three axis-switching for 2:1 aspect ratio elliptic jet and found that the mass entrainment of the elliptic jet was several times higher than that of circular jet. Quinn [26] observed two axis-switching and found that the jet attains an axisymmetric shape at about 30 equivalent slot diameters downstream of the exit plane. Menon and Skews [27] found that the phenomenon of axis-switching in elliptical nozzles was exacerbated on increasing the pressure ratio.

From the above discussions, it is evident that, jet plays a dominant role in many disciplines of engineering. Also, the jet needs to be controlled to serve efficiently for any specific purpose for which it is employed. Thus, jet control becomes an inevitable part of jet research. However, even though a quantum of information is available in literature, accounting for core length reduction with triangular tabs and with triangular tabs without holes, the physics of the mixing enhancement caused by these passive controls are not deeply probed into, especially in the sonic and supersonic regimes. With this in mind, the present investigation aims at evaluating the efficacy of passive control in the form of triangular tabs with and without holes, on mixing characteristics of supersonic jets to apprehend the governing flow physics and to capture the flow structure, in the presence of different levels of under expansion at the nozzle exit.

Supersonic jets issuing from convergent divergent elliptic nozzle with and without control, at under expanded and over expanded conditions in the range of nozzle pressure ratio (NPR) from 3 to 6 were investigated. The equivalent diameter was 12.7 mm in all the cases. Convergent elliptic nozzle of Aspect Ratio AR 3 was studied. The effect of following tabs on jet flow was studied: Triangular tabs on major axis, Triangular tabs on minor axis, Triangular tabs having circular hole on major axis, Triangular tabs having circular hole on minor axis, Triangular tabs having triangular hole on major axis, Triangular tabs having triangular hole on minor axis.

The blockage due to the tabs, defined as the ratio of the projected area of the tabs normal to the nozzle axis to the nozzle exit area, was 5%. Both quantitative and qualitative studies were carried out for all the combinations of the flow and geometric parameters of the present study. On the quantitative side, the centerline pitot pressure decay, pressure profiles in the directions along and normal to the tabs were carried out. The waves prevailing in the jet field with and without controls have been visualized using shadowgraph technique.

Experimental Setup and Procedure
Experimental Setup
The experiments were conducted in the open jet facility at the high-speed aerodynamics laboratory, Indian Institute of Technology, India. The test facility consists of Compressor, Storage tanks and an open jet test facility. A schematic diagram of the open jet facility laboratory is shown in Figure-6.
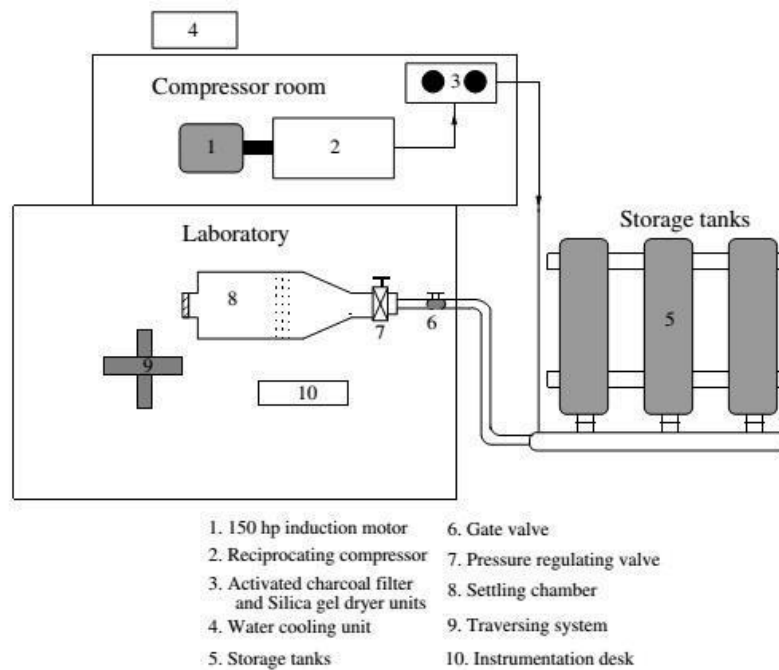
Fig-6: Layout of the open jet facility laboratory

1. 150 hp induction motor
2. Reciprocating compressor
3. Activated charcoal filter and Silica gel dryer units
4. Water cooling unit
5. Storage tanks
6. Gate valve
7. Pressure regulating valve
8. Settling chamber
9. Traversing system
10. Instrumentation desk

Air Supply System

The compressed air supply system consists of a two stage, reciprocating compressor, capable of delivering 360 cubic ft / min of air at a pressure of 500 psi. The compressed air is cooled by passing through an inter-cooler and then fed to a pre-filter consisting of porous stone candles to remove solid contaminants and oil droplets. An activated carbon filter is used for finer filtering. The compressed air is dried in a dual-tower semi-automatic silica gel dryer. A portion of the dried air is heated and used for alternate reactivation of each tower. A diaphragm type back pressure valve operated by a pressure relief pilot, which permits the air dryer to operate at 500 psi as the pressure in the receivers builds up from atmospheric to the required storage pressure. The air is stored in three tanks, having a total capacity of 3000 ft^3. The tunnel control section includes a gate valve followed by a pressure regulating valve. The pressure regulating valve is connected to a mixing tube of 3 inches diameter and then to a settling chamber.

Open Jet Test Facility

The experiments were conducted using an open jet facility which consists of a cylindrical settling chamber connected to high pressure storage tanks. Figure-7 shows a schematic sketch of the free jet test facility. The air enters the settling chamber through the tunnel section with a gate valve followed by a pressure regulating valve and a mixing length tube of 3 inches diameter. The settling chamber is connected to the mixing tube by a wide-angle diffuser followed by three screens or closely meshed grids set 3 cm apart for minimizing turbulence at the nozzle inlet. These screens are inserted in the settling chamber. The settling chamber has a constant area circular section of 300 mm inside diameter and 600 mm length. The settling chamber has tapings for stagnation pressure and temperature measurements. The test models are fixed at the end of the settling chamber by a slot holder arrangement, which is a short pipe like protrusion with embedded O-ring to prevent leakage. Model to be studied is placed over the O-ring, over which an annular retaining sleeve with internal threads is screwed tightly.
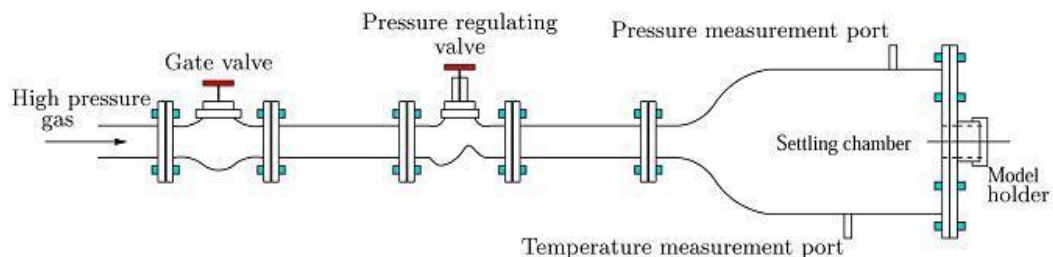

Fig-7: Schematic diagram of a free jet test facility

The settling chamber total pressure *P0*, which was the controlling parameter in this investigation, was maintained constant during a run by controlling the pressure regulating valve. The stagnation pressure *P0* level in the settling chamber gives the different nozzle pressure ratios NPR, defined as the ratio of stagnation pressure to the back pressure ($P0/p_b$) required for any study. The settling chamber temperature is the same as the ambient temperature and the back pressure is the ambient pressure into which the jets were discharged. The ambient temperature of the room was almost constant within ±0.50 C during one experimental run. The stagnation pressure was maintained with an accuracy of ±0.1%. During the experimental runs, the settling chamber pressure was measured by a pressure transducer. A thermometer measured the room temperature and the mercury barometer placed in the laboratory and averaged over the duration of experiment measured the day-to-day changes in ambient pressure p_a.

Instrumentation for Pressure Measurement
Pressure Probe

In the present investigation, the pressure-sensing probe used was the conventional pitot probe. The pitot probe has been one of the most useful and widely used instruments in experimental fluid mechanics. The accuracy of it depends on its shape, the Reynolds number, the magnitude of transverse shear, turbulence intensity and length scale, the orientation with respect to the mean flow direction and the Mach number.
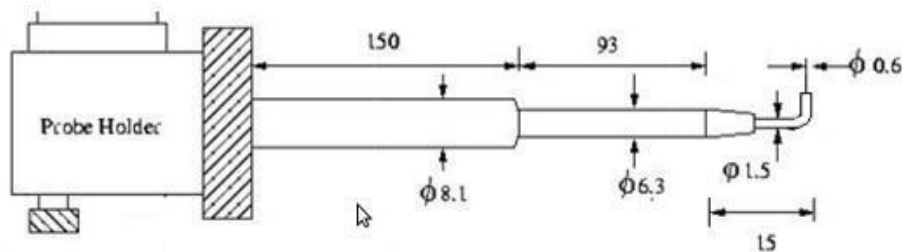

Fig-8: Schematic diagram of the pitot probe

Schematic sketch of the pitot probe and its attachment system is shown in Figure 8. The Pitot probe used was of outer diameter 0.6 mm and inner diameter 0.4 mm. Thus, the ratio of nozzle exit area to the probe area is 277.77, which is well above the limit of 64 for regarding the probe blockage negligible [1]. Further, the Reynolds numbers based on the equivalent diameter *D* were 2.96×10^5 and 7.39×10^5, respectively, for the minimum and maximum NPRs of 2 and 5 of the present investigation. These values are much higher than the troublesome Reynolds number of 500. Therefore, the viscous effects on pitot pressure measurements are insignificant for the present investigation. Another point to be noted in pitot pressure measurements is that, in supersonic regime what the probe measures is the total pressure behind the bow shock that stands ahead of the probe. Thus, it is not the actual total pressure. If the actual total pressure is required one has to correct for the pressure loss across the shock. Since the supersonic jet core is wave dominated, the Mach number in the core varies from point to point and also the shocks in different cells are of varying strength. Therefore, no attempt is made to correct the measured total pressure for shock loss. It has to be emphasized that in supersonic regions there is some measurement error due to probe interference with shock structure and so the measured pressure data in supersonic regions should be considered only qualitative and good enough for comparative study.

In all the pressure measurements, the sensing probe stem was oriented parallel to y-axis with the sensing probe facing the jet *x*-axis. The pitot probe is mounted on a three-dimensional traverse as depicted in Figure-9. The traverse has six degrees of freedom, which also include a probe-yawing mechanism. The traverse has linear resolution of 0.1 mm in all the three dimensions i.e., the positioning accuracy of the probe was within ±0.1 mm in all the three axes X, Y and Z.

Fig-9: A view of the jet facility

Pressure Transducer and Application Software

The pitot pressure sensed by the probe was measured using a PSI model 9010, 16-channel pressure transducer (interface with a Pentium 4 computer loaded with VI based software for data acquisition). The model 9010 transducer is capable of measuring pressures up to 250 psi, which is approximately 17 atm. The transducer also has a facility to choose the number of samples to be averaged, by means of dip-switch settings. The accuracy of the transducer (after re-zero calibration) is specified to be ±0.15% full scale. Also, transducer off-set errors were eliminated by performing a re-zero calibration prior to every run. The system 9010 intelligent pressure scanner is a pressure measuring device intended for use in test and production environments. It consists of 16-channels and is working in differential mode. It has an asynchronous RS422/485 host communication interface. It also has a standard RS-232 diagnostic interface that may also be used as host interface. The "Optomux" command set is used to send commands and receive response from all ports. It may be configured to communicate in the multi-drop network communication always at selected baud rate, using the "Optomux" protocol. The multi-drop communication always operates with no parity, 8-bit data bits and 1 stop bit. The default baud rate is 9600 and changes to the baud rate can be made using special procedure via the DIP switch used to select the node address during initialization at power up. During this special baud rate selection procedure, the number of averages used during the data acquisition is also selected. The application software developed using the Lab VIEW performs all the required functions like initialize, reset, re-zero calibration, and read pressure. The application software links the host computer to the pressure scanner via RS-232 communication.

Experimental Models and Tabs Attachment

Supersonic jets issuing from convergent divergent elliptic nozzle with and without control, at under expanded and over expanded conditions in the range of nozzle pressure ratio NPR from 3 to 6 were investigated. The equivalent diameter *D*, defined as the diameter of a circular nozzle of same exit area as the elliptic model exit area was 12.7 mm, in all the cases. Convergent elliptic nozzle of Aspect Ratio *AR* = 3 was studied. The blockage due to the tabs, defined as the ratio of the projected area of the tabs normal to the nozzle axis to the nozzle exit area, was 5%. Different tabs are shown in Figure-10.

Fig-10: The tabs from left to right are Circular hole on triangular major tabs, Circular hole on triangular minor tabs, Triangular hole on triangular minor tabs, Triangular hole on triangular major tabs, Minor tabs, and Major tabs

Fig-11: Mach 1.5 convergent-divergent elliptical nozzle of Aspect Ratio 3

The Mach 1.5 convergent divergent nozzle without any tabs is shown in Figure-11. The nozzle configuration with triangular hole on major tabs is depicted in Figure-12.

Fig-12: Nozzle configuration with triangular hole on minor tabs

Experimental Procedure
Centerline Pitot Pressure Decay

The centerline pitot pressure distributions for supersonic jet Mach 1.5 at different levels of expansion were measured by placing the pitot probe along the jet axis (*x*-axis), from the exit of the nozzle in the downstream direction. The pitot probe was moved along the jet axis, at intervals of 1 mm, up to 15 *D*. The measured stagnation pressure corresponds to the stagnation pressure behind the standing bow shock in front of the pitot tube, in the supersonic regions of the jet.

Pitot Pressure Profiles

The pitot pressure measurements were also carried out in the lateral directions (*Y*- and *Z*-axis) for plotting pressure profiles. Later, the pitot pressure p_t

measured is divided by the stagnation pressure of the settling chamber and plotted against the nondimensionalized lateral distances, *Y/D* and *Z/D*. The pressure survey was done at different axial locations for different nozzle pressure tube.

Shadowgraph System

In supersonic flows, the large density variations lead to variations in optical refractive index of the light. Shadowgraphs are usually considered mainly useful for revealing strong density gradients of the flow. Shadowgraph system at the open jet facility of IIT Kanpur was used in the present study for visualizing wave patterns in the jet field with and without controls. The flow pattern was filmed using a shadowgraph system with a Helium spark arc light source in conjunction with 150 mm concave mirror. The light source was collimated by the condenser lens and was then brought to the concave mirror. The parallel beam from the mirror was made to pass through the test-section and projected on the screen.

The shadowgraph images of shock-train on the screen were recorded directly with a still camera. The focal length of the mirror is 1.6 m. The arrangement of mirror and light source are shown in Figure 13. When flow takes place through the test- section the light beam will be refracted wherever there is a density gradient. However, if the density gradient everywhere in the test-section is constant, all light rays would deflect by the same amount, and there would be no change in the illumination of the picture on the screen. Only when there is a gradient in density gradient, there will be tendency for light rays to converge or diverge. In other words, the variations in illumination of the picture on the screen are proportional to the second derivative of the density.
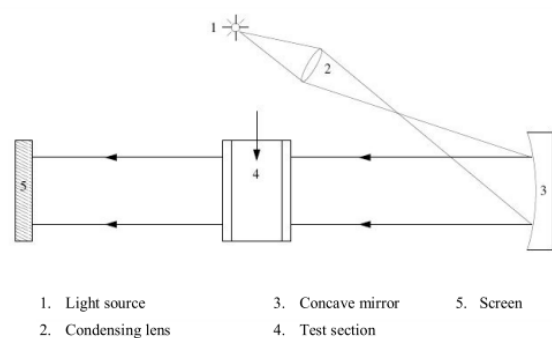

| 1. Light source | 3. Concave mirror | 5. Screen |
| 2. Condensing lens | 4. Test section | |

Fig-13: Schematic diagram of light source and mirror

RESULTS AND DISCUSSION

One of the fascinating features of elliptical jet is its geometry itself. In accordance to vortex theory an elliptical nozzle would shed mixing promoting vortices of continuously varying size from one end of the minor axis to the nearest end of the major axis. This continuous variation in mixing promoting vortices would enhance jet mixing considerably. Thus, elliptical

jets are found to be superior as compared to an identical circular jet from aerodynamic mixing point of view. Because of his interesting features, many researchers focus their attention on elliptical jet study in the past but what was claimed as elliptical jet was jet issuing form nozzles of circular cross section from entry to exit, with a plate of elliptical opening attached at the opening. In the recent past elliptical jets issuing from actual elliptical nozzles (convergent as well as convergent divergent nozzle) of elliptical cross section from inlet to exit has been studied [16] and [28]. It is fascinating that these studies cover a range of Mach numbers from sonic to supersonic and both uncontrolled and controlled elliptic jets are studied in detail. To investigate this interesting aspect of ventilation effect at the tabs on the mixing promotion. In the present study attention is focused on the control of a Mach 1.5, elliptical jet issuing from elliptical convergent divergent nozzle of aspect ratio 3. Triangular tabs with ventilation on the form of circular and triangular holes, without ventilation located along the major and minor axis at the nozzle exit were studied. Two identical tabs of geometrical blockage 2.5% each were used in the present study. All the tabs were made of 1 mm brass sheet.

The mixing promoting capability of plain and ventilated triangular tabs were investigated at the NPRs 3, 4, 5, and 6 for Mach 1.5 nozzle. NPR 3 is in over expanded state with an overexpansion level of 18.28% at nozzle exit. NPR 4, 5, 6 are in under-expansion state with under-expansion level of 8.96%, 36.20%, and 63.44% respectively. The performance of controlled jet was compared with uncontrolled jets for all the NPRs.

The measured data consists of pitot pressure distribution along the data axis, from the nozzle exit to 15 D and the pitot pressure distribution in the direction of major and minor axis at different axial location for all the combination of the geometric and flow parameters of the controlled and uncontrolled jets. The pitot pressure was made nondimensionalized by dividing with the settling chamber pressure. The length along the data axis X, along the Y and along the minor axis Z are made nondimensionalized by dividing with the equivalent diameter of the nozzle exit.

Centerline Pressure Decay

It is well known that centerline pressure decay CPD is an authentic mean to analyze the jet mixing. The CPD can be used to quantify the core length, the characteristic decay rate and the far field or fully developed field decay. It is essential to note that pitot's pressure measured in supersonic flow can't be converted to Mach number of velocity because supersonic jet is essentially dominated by waves of different family, which are non-linear, and the different zones in supersonic regime are non-simple [1].

The CPD for the controlled and uncontrolled jets at NPR 3 are presented in Figures 14 and 15. Figure 14 compares the CPD for uncontrolled and controlled jets with tabs along the major axis and Figure 15 presents the CPD results for uncontrolled and controlled jets with tabs along the minor axis. From these results it is explicitly seen that in the presence of adverse pressure gradient, the mixing promotion caused by tabs along minor axis is appreciably greater than that of uncontrolled jets, whereas the tabs along major axis results in reduced mixing compared to the uncontrolled jets in the near field.

A closer look over vortex dynamics might throw some light over this impressive mixing caused by tabs along minor axis. From vortex dynamics it is known that the mixing promoting vortices shed by a control such as tab and from nozzle edge should not interact just at the nozzle exit and loose its vorticity (strength). For this there should be some spacing between the sharp corners formed by fixing the tabs at the nozzle exit. This would ensure that the mixing promoting vortices would leave the nozzle exit without interacting and losing their strength before getting into mixing promoting action. For the present geometry of AR 3 elliptical opening, fixing the tabs at the end of minor axis appears to provide this favorable environment for mixing promotion. Furthermore, tabs at the ends of minor axis proves to be adverse to this favorable environment for mixing promotion. The core length of jets with tabs along minor axis is shorter than the core length of jets with tabs along major axis. Among jets with triangular minor tabs and circular hole on minor tabs, the triangular minor tabs possess slightly shorter core of about 0.5 D when compared to 0.6 D of circular hole minor tabs. At this Nozzle pressure ratio, the triangular hole on minor tabs has longer core than the jets with triangular minor tabs and circular hole minor tabs. It is seen in Figure 1that the triangular minor tabs and circular hole minor tabs jet decay are almost at the same rate from 1D onwards. In case of jets with tabs along major axis, the triangular major tabs are found to possess shorter core than the other two jets.
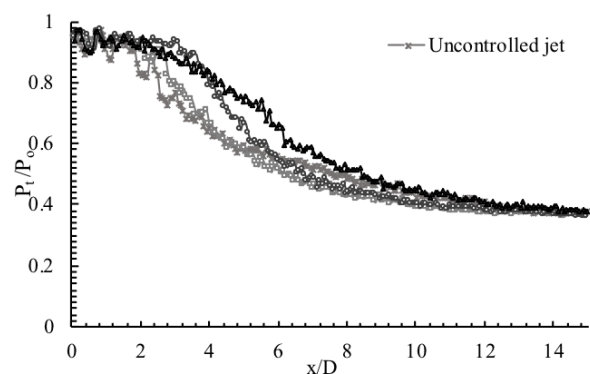

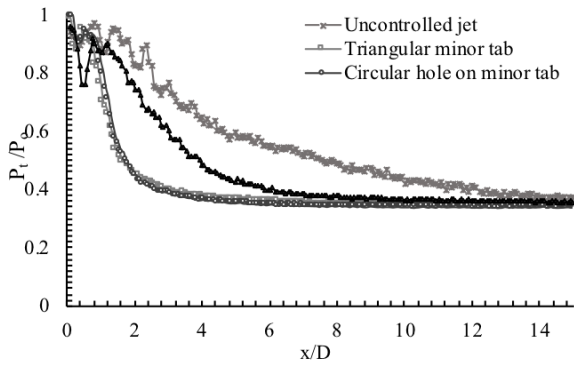**Fig-14: Centerline pressure decay, NPR3, Major-tabs**
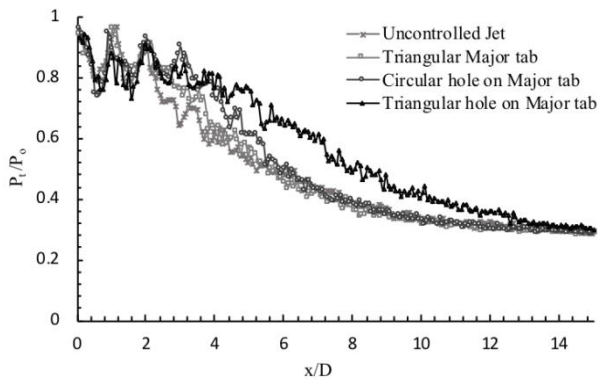
Fig-15: Centerline pressure decay, NPR3, Minor tabs

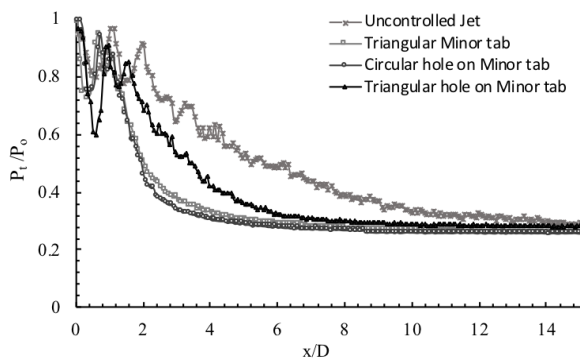**Fig-16: Centerline pressure decay, NPR4 (under expanded), Major-tabs**

Fig-17: Centerline pressure decay, NPR4 (under expanded), Minor tabs

Fig-18: Centerline pressure decay, NPR5 (under expanded), Major-tabs

Fig-19: Centerline pressure decay, NPR5 (under expanded), Minor tabs

uncontrolled jets like in case of NPR3 to become fully developed at about 9*D*. At this NPR also, the core lengths of controlled jets are shorter than the uncontrolled jets except the jet with triangular hole on major tabs where the core length is longer than the uncontrolled jet. As the NPR increases from 4 to 5 the favorable pressure gradient also increases at the nozzle exit. It is seen that except the jet with triangular hole on major tabs, the other controlled jets are found to possess shorter core than the uncontrolled jets. At this NPR also, the decay of jets with tabs along major axis is not appreciable compared to uncontrolled jet.
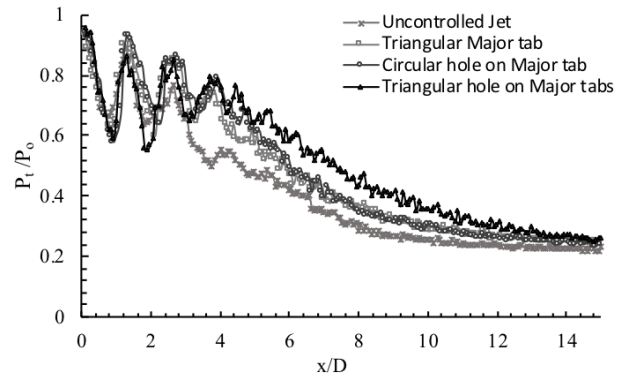
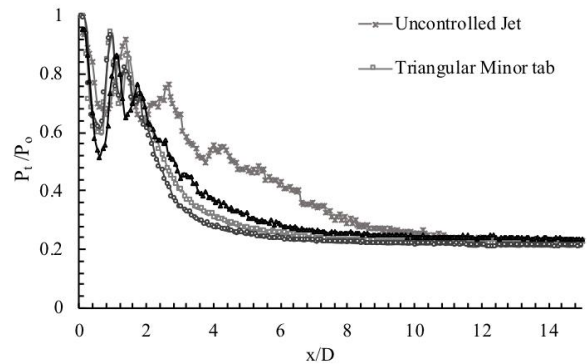Figures 16 - 21 show centerline pressure decay minor and major-tabs with increase in NPR from 3 to 4, the adverse pressure gradient at the nozzle exit comes down to marginal favorable pressure gradient as the correctly expanded NPR for Mach 1.5 jet is 3.67. At this NPR also, the jets with tabs along minor axis show enhanced mixing characteristics in all the three zones of the jet, namely core, characteristic decay and fully developed zones. The core lengths of jet with tabs along minor axis is shorter than the core lengths of jets with tabs along major axis. At this NPR the triangular major tabs and circular hole on minor tabs jets possess the same core length and decay of both the jets area almost similar. They become fully developed at about 4*D* whereas the jet with triangular hole on minor tabs became fully developed at about 6*D*. The jets with tabs along major axis decay slightly faster than the

The jets with tabs along the minor axis decays almost at the same rate from 2 *D* to become fully developed at about 5 D. At NPR 5 also the jets with tabs along minor axis performs better than the jets with tabs along major axis.
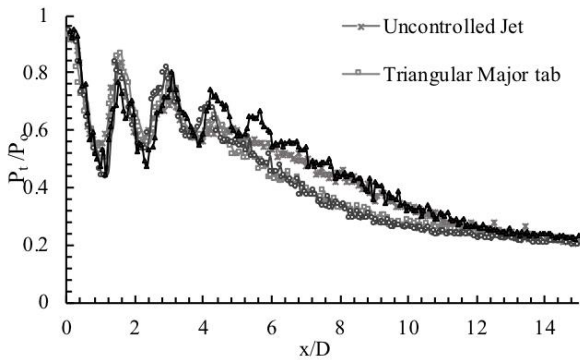
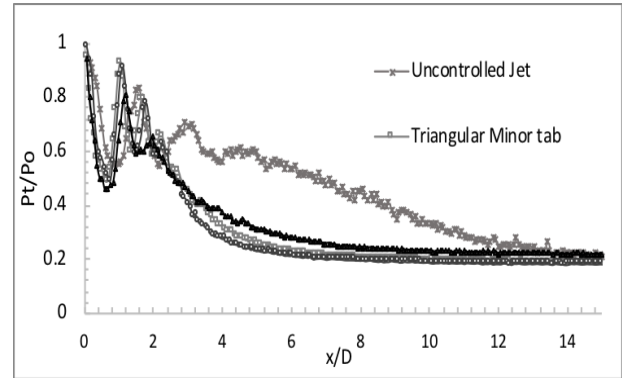**Fig-20: Centerline pressure decay, NPR6 (under expanded), Major-tabs**

Fig-21: Centerline pressure decay, NPR6 (under expanded), Minor-tabs

As NPR increases from 5 to 6, the level of under expansion increases indicating increase in favorable pressure gradient at the nozzle exit. At NPR 6, the jets with tabs along major and minor axis behaves like that of jet at NPR 5. The jets with tabs along minor axis exhibit shorter core that jets with tabs along major axis. The jets with tabs along minor axis become fully developed at about $6D$ whereas the jets with tabs along major axis become fully developed at about $11D$ only.

Likely in other NPRs the jets with tabs along major axis enjoy superior mixing characteristics as compared to jets with tabs along major axis. Core length of jets with tabs along major and minor axis and uncontrollable jets are shown in Table-1.

Table-1: Core Length of jets with Equivalent Nozzle Diameter

NPR	Core Length of jets/ Equivalent Nozzle Diameter							
	Uncontrolled jets		Triangular tabs		Triangular tabs with circular hole		Triangular tabs with Triangular holes	
	Major	Minor	Major	Minor	Major	Minor	Major	Minor
3	3.01	3.01	2.48	0.52	3.08	0.60	2.63	1.13
4	4.32	4.30	2.23	1.13	4.70	1.13	5.60	1.50
5	4.37	4.37	3.84	1.5o	4.00	1.80	5.42	1.73
6	4.97	4.97	4.60	2.26	4.30	2.33	5.65	1.88

Pitot Pressure Profiles

One of the problems associated with jet control is that the asymmetry might become more for the controlled jet. This is because of the intense vortex activity in the near field, causing the jet to become oscillatory and unsteady. Therefore, it is essential to assess this aspect. To study this, pitot pressure variation for controlled jets were measured and compared for all the combination of the parameters of the present investigation. As the nozzle is elliptic in the present study, the profile plots were taken along major and minor axis of the jet at different axial locations. The pressure profile for the uncontrolled jets for NPRs 3 to 6 is shown in Figure-22. It is seen that at all the NPRs the jet spread along the major axis is large compared to the jet spread along the minor axis up to $4D$. From $7D$ onwards, the minor axis jet spread is larger compared to the major axis jet spread, indicating that the uncontrolled jet has switched its axis at all the NPRs studied.

The pressure profiles at $0.5D$, $1D$ and $2D$ at NPR 3 shows off center peaks because of the shock cells present in the core of the jet. From $4D$ onwards, the off-center peaks disappear reflecting the end of core length which is also supported by CPD plots at NPR3.

At NPR 4 onwards, the off-center peaks are visible up to $4D$ indicating the presence of core length up to $4D$. For all the NPRs from $7D$ onwards the pressure profile shows a single peak which is due to the measurement taken at characteristic decay zone. At about $10D$ the jets show the tendency to become fully developed.

The pressure profile plots for jets with triangular major tabs, circular hole triangular major tabs, and triangular hole triangular major tabs. It is seen that the presence of tabs along major axis has resulted in the fastest spread of jet along minor axis when compared to jet spread along major axis at all the NPRs. As a result, the jets with tabs along major axis have switched in axis at all the NPRs studied. Like uncontrolled jet the jets with tabs along major axis exhibits off center peaks due to the presence of core also the centerline pressure values of the jets with tabs along major axis at all the axial location which is further supported by the discussions made from CPD plot. Whereas when compared to uncontrolled jets, the jets with tabs along major axis shows centerline pressure values of lesser magnitude. The jets with tabs along major axis also show a tendency to become fully developed from $10D$ inwards. Also, the variation among the pressure profiles for jets with triangular major tabs, circular hole on triangular major tabs and

triangular hole on triangular major tabs is les because they almost exhibit similar centerline pressure decay at all the NPRs.
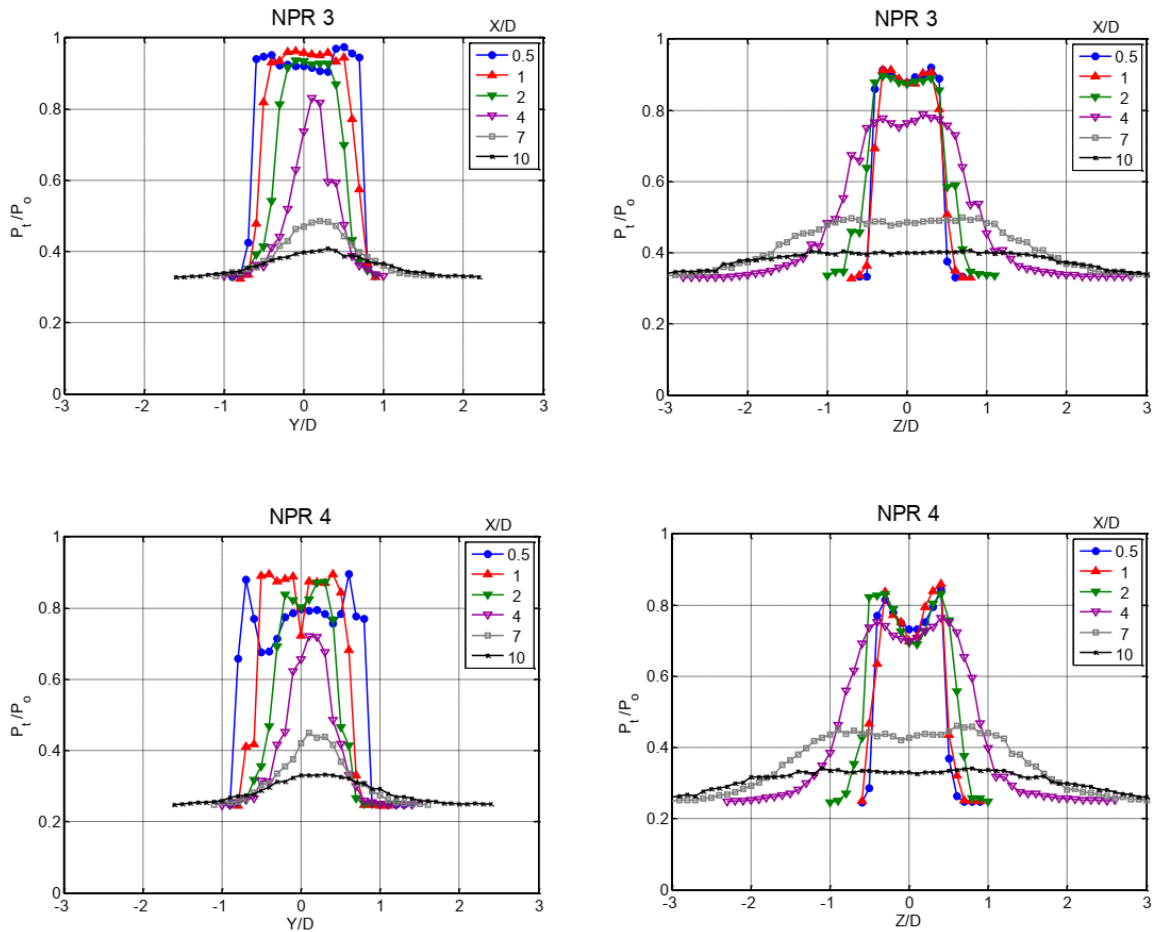

Fig-22: Pitot pressure profiles of uncontrolled jet at different axial locations

Optical Flow Visualization

To study the shock cell structures in the core of the under expanded and over expanded supersonic jets, shadowgraph pictures were taken at different NPRs. The images were taken by viewing along the XY-plane (major-axis plane) and XZ-plane (minor-axis) plane and shown in Figures 23-25. These shadowgraph pictures reveal the difference in the nature of the shock cell structure along XZ- and XY-plane.

The non-symmetric shock cell structure in the major- and minor-axis plane of the elliptic jets is due to the fact that the expansion and shock waves emerge at different angles from the nozzle exit along the two planes of the jet. The distinct nature of pitot pressure prof0iles along major and minor-plane is evident from these shock cell structures. These shock structures expand along minor-axis plane and contract along major-axis plane.
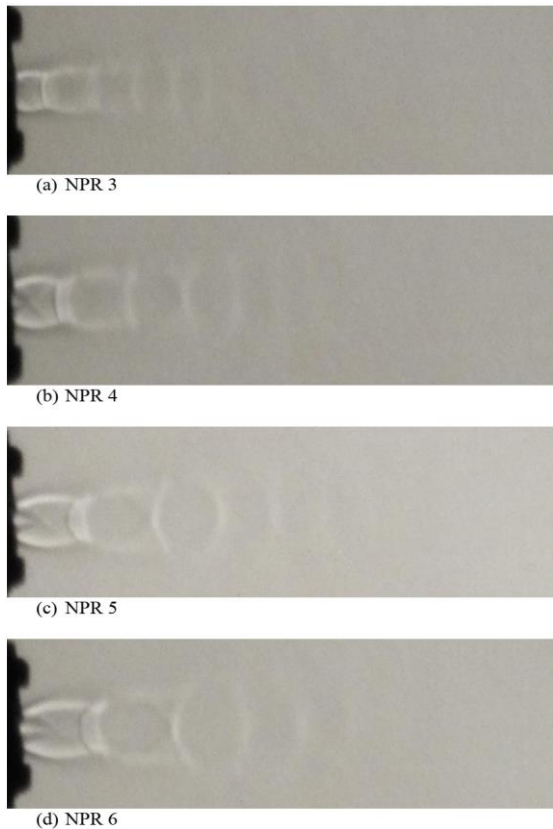
(a) NPR 3

(b) NPR 4

(c) NPR 5

(d) NPR 6

Fig-23: Shadowgraph visualization along the x-z plane for the jet controlled with circular hole on major tabs

(a) NPR 3

(b) NPR 4

(c) NPR 5

(d) NPR 6

Fig-24: Shadowgraph visualization along the x-y plane for the jet controlled with triangular hole on major tabs
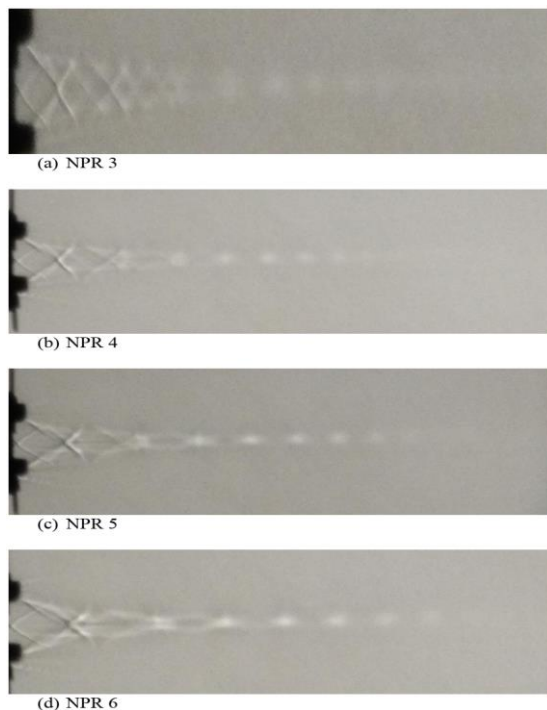

(a) NPR 3

(b) NPR 4

(c) NPR 5

(d) NPR 6

Fig-25: Shadowgraph visualization along the x-z plane for the jet controlled with triangular hole on major tabs

Shadowgraph picture for the jet controlled with plain triangular tab along minor axis are shown in [29]. It is seen in [29] that at all the levels of expansion the tab essentially tends to bifurcate the jet. The bifurcation of the jet leads to widening of the jet as seen in the as seen in the shadowgraph picture. When viewed along the major axis it is seen in [29] that the tabs could able to weaken the waves present in the core compared to the uncontrolled jet. For circular hole on triangular tab it is interesting to see that there is no tendency for jet to bifurcate the shock from the opposite edge of the jet boundary and over to the jet axis. This may be because of the near field mixing due to the additional vortices shed from the circular perforation influencing the jet away from the centerline.

In triangular hole on tabs visualization it is interesting to see that the triangular hole on triangular tab could able to introduce additional wave in jet axis in both the direction. An interesting aspect observed for this case is that viewing in the major direction exhibits nonlinear waves whereas viewing in the minor direction reveals waves of almost linear nature.

CONCLUSIONS
In the present study, the effect of ventilation on tabs was investigated experimentally in the presence of favourable and adverse pressure gradient at the nozzle exit. The experimental model used in the present investigation was Mach 1.5 elliptic convergent divergent nozzle of aspect ratio 3. The tabs used in present investigation were triangular tabs, triangular hole on triangular tabs, and circular hole on triangular tabs. The quantitative and qualitative results of the present investigation on the mixing promoting

efficiency of ventilated tabs used in the study, clearly demonstrate that:

- Plain triangular minor tabs are found to be effective in enhancing the mixing compared to ventilated tabs at the level of overexpansion (NPR3) and moderately underexpansion (NPR 4,and NPR5). The shorter core lengths followed by a rapid decay of pitot pressure demonstrate the superiority of plain triangular tabs at these NPRs
- Ventilated triangular tabs with circular holes on major tabs and triangular ventilation on minor triangular tabs are found to be effective in enhancing the mixing at higher NPR (NPR 6).
- Ventilated triangular tabs with triangular holes on major tabs is found effective in enhancing mixing at lower NPR (NPR 3).

REFERENCES

1. Rathakrishnan E. "Applied Gas Dynamics," John Wiley and Sons (Asia) Pte Ltd, 2010.
2. Miller RS, Madnia CK, Givi P. Numerical simulation of non-circular jets. Computers & fluids. 1995 Jan 1;24(1):1-25.
3. Quinn WR. Experimental study of the near field and transition region of a free jet issuing from a sharp-edged elliptic orifice plate. European Journal of Mechanics-B/Fluids. 2007 Jul 1;26(4):583-614.
4. Grinstein FF, Gutmark E, Parr T. Near field dynamics of subsonic free square jets. A computational and experimental study. Physics of Fluids. 1995 Jun;7(6):1483-1497.
5. Gutmark E, Schadow KC, Wilson KJ. Subsonic and supersonic combustion using noncircular injectors. Journal of propulsion and power. 1991 Mar;7(2):240-249.
6. Clement S, Murugan KN, Rathakrishnan E. Superiority of elliptical jets. J Institution of Engineers (India). 2005 May;86:1-7.
7. Wei CY, Drallmeier J, Isaac K. Analysis of primary atomization in supersonic coaxial systems. In28th Joint Propulsion Conference and Exhibit 1992 Jul; 3236.
8. Gutmark EJ, Schadow KC, Yu KH. Mixing enhancement in supersonic free shear flows. Annual Review of Fluid Mechanics. 1995 Jan;27(1):375-417.
9. Papamoschou D, Debiasi M. Noise measurements in supersonic jets treated with the Mach wave elimination method. AIAA journal. 1999 Feb;37(2):154-60.
10. Brown GL, Roshko A. On density effects and large structure in turbulent mixing layers. Journal of Fluid Mechanics. 1974 Jul;64(4):775-816.
11. Dimotakis PE, Brown GL. The mixing layer at high Reynolds number: large-structure dynamics and entrainment. Journal of Fluid Mechanics. 1976 Dec;78(3):535-560.
12. Bernal LP, Roshko A. Streamwise vortex structure in plane mixing layers. Journal of Fluid Mechanics. 1986 Sep;170:499-525.
13. Crow SC, Champagne FH. Orderly structure in jet turbulence. Journal of Fluid Mechanics. 1971 Aug;48(3):547-591.
14. Sforza PM, Steiger MH, Trentacoste N. Studies on three-dimensional viscous jets. AIAA journal. 1966 May;4(5):800-806.
15. Gutmark E, Schadow KC, Parr TP, Hanson-Parr DM, Wilson KJ. Noncircular jets in combustion systems. Experiments in Fluids. 1989 Feb 1;7(4):248-258.
16. Kumar PA, Rathakrishnan E. Corrugated triangular tabs for supersonic jet control. Proceedings of the Institution of Mechanical Engineers, Part G: Journal of Aerospace Engineering. 2014 May;228(6):831-845.
17. Koshigoe S, Gutmark E, Schadow KC, Tubis A. Initial development of noncircular jets leading to axis switching. AIAA journal. 1989 Apr;27(4):411-419.
18. Gutmark E, Schadow KC, Bicker CJ. Near acoustic field and shock structure of rectangular supersonic jets. AIAA journal. 1990 Jul;28(7):1163-1170.
19. Krothapalli A, Hsia Y, Baganoff D, Karamcheti K. The role of screech tones in mixing of an underexpanded rectangular jet. Journal of Sound and Vibration. 1986 Apr 8;106(1):119-143.
20. Srinivasan K, Rathakrishnan E. Studies on underexpanded rectangular slot jets. Journal-Aeronautical Society of India. 2001;53(1):39-43.
21. Schadow KC, Gutmark E, Koshigoe S, Wilson KJ. Combustion-related shear-flow dynamics in elliptic supersonic jets. AIAA journal. 1989 Oct;27(10):1347-1353.
22. Mitchell DM, Honnery DR, Soria J. Near-field structure of underexpanded elliptic jets. Experiments in fluids. 2013 Jul 1;54(7):1578.
23. Yoon JH, Lee SJ. Investigation of the near-field structure of an elliptic jet using stereoscopic particle image velocimetry. Measurement Science and Technology. 2003 Oct 6;14(12):2034-2046.
24. Hussain F, Husain HS. Elliptic jets. Part 1. Characteristics of unexcited and excited jets. Journal of Fluid Mechanics. 1989 Nov;208:257-320.
25. Ho CM, Gutmark E. Vortex induction and mass entrainment in a small-aspect-ratio elliptic jet. Journal of Fluid mechanics. 1987 Jun;179:383-405.
26. Quinn WR. On mixing in an elliptic turbulent free jet. Physics of Fluids A: Fluid Dynamics. 1989 Oct;1(10):1716-22.
27. Menon N, Skews BW. Shock wave configurations and flow structures in non-axisymmetric underexpanded sonic jets. Shock Waves. 2010 Jun 1;20(3):175-90.
28. Chauhan V, Aravindh Kumar SM, Rathakrishnan E. Mixing characteristics of underexpanded elliptic sonic jets from orifice and nozzle. Journal of Propulsion and Power. 2015 Jan 9;31(2):496-504.
29. Dadhich D. Jet control with ventilated triangular tabs, M. Tech. Thesis, Indian Institute of Technology, Kanpur, 2015.